0026-895X/04/6603-601–611$20.00
MOLECULAR PHARMACOLOGY
Copyright © 2004 The American Society for Pharmacology and Experimental Therapeutics
Mol Pharmacol 66:601–611, 2004

Vol. 66, No. 3
224/110192
Printed in U.S.A.

Identification of the $P2Y_{12}$ Receptor in Nucleotide Inhibition of Exocytosis from Bovine Chromaffin Cells

Steven J. Ennion, Andrew D. Powell, and Elizabeth P. Seward

Department of Cell Physiology and Pharmacology, University of Leicester, Leicester, United Kingdom (S.J.E.); Department of Pharmacology, University of Bristol, Bristol, United Kingdom (A.D.P.); and Department of Biomedical Sciences, University of Sheffield, Sheffield, United Kingdom (E.P.S.)

Received March 8, 2004; accepted May 28, 2004

ABSTRACT

Nucleotides are released from bovine chromaffin cells and take part in a feedback loop to inhibit further exocytosis. To identify the nucleotide receptors involved, we measured the effects of a range of exogenous nucleotides and related antagonists on voltage-operated calcium currents (I_{Ca}), intracellular calcium concentration ($[Ca^{2+}]_i$), and membrane capacitance changes. In comparative parallel studies, we also cloned the bovine $P2Y_{12}$ receptor from chromaffin cells and determined its properties by coexpression in *Xenopus laevis* oocytes with inward-rectifier potassium channels made up of Kir3.1 and Kir3.4. In both systems, the agonist order of potency was essentially identical (2-methylthio-ATP $\approx$ 2-methylthio-ADP $\gg$ ATP $\approx$ ADP $>$ UDP). $\alpha\beta$-Methylene-ATP and adenosine were inactive. UTP inhibited I_{Ca} in chromaffin cells ($pEC_{50} = 4.89 \pm 0.11$) but was essentially inactive at the cloned $P2Y_{12}$ receptor. The relatively nonselective P2 antagonist pyridoxal-phosphate-6-azophenyl-2′,4′ disulfonic acid blocked nucleotide responses in both chromaffin cells and *X. laevis* oocytes, whereas the $P2Y_{12}$- and $P2Y_{13}$-selective antagonist N^6-(2-methylthioethyl)-2-(3,3,3-trifluoropropylthio)-β,γ-dichloromethylene ATP (ARC69931MX) blocked responses to ATP in both chromaffin cells and *X. laevis* oocytes but not to UTP in chromaffin cells. These results identify the $P2Y_{12}$ purine receptor as a key component of the nucleotide inhibitory pathway and also demonstrate the involvement of a UTP-sensitive $G_{i/o}$-coupled pyrimidine receptor.

Given the profusion of P2 nucleotide receptors in the nervous system and the many pathways for nucleotide release, the potential for extracellular nucleotides to play a major modulatory role in neurotransmission is high. Because of their structure and signaling mechanisms, P2 receptors are classified either as ligand-gated $P2X_{1-7}$ cation channels or as metabotropic $P2Y_1$, $P2Y_2$, $P2Y_4$, $P2Y_6$, $P2Y_{11}$, $P2Y_{12}$, $P2Y_{13}$, $P2Y_{14}$, and $P2Y_{15}$ receptors coupled to heterotrimeric G proteins (North, 2002; Abbracchio et al., 2003; Inbe et al., 2004). Activation of P2X receptors by ATP leads directly to membrane depolarization and calcium entry both via the P2X channels themselves and by the subsequent activation of voltage-operated calcium channels (VOCCs) (North, 2002). P2Y receptors have a wider agonist profile than the P2X receptors responding to purines, pyrimidines, and UDP-glucose. These receptors can be divided into two subgroups based on their molecular structure and coupling to Gα-subunits, with $P2Y_{12}$, $P2Y_{13}$, and $P2Y_{14}$ making up one group that signals via PTX-sensitive $G_{i/o}$ proteins and $P2Y_1$, $P2Y_2$, $P2Y_4$, $P2Y_6$, $P2Y_{11}$, and $P2Y_{15}$ making up the second group that couples to phospholipase C and G proteins of the G_q class (Abbracchio et al., 2003; Inbe et al., 2004).

In the sympathetic nervous system, the effects of presynaptic purine receptors on neurotransmission have been well-documented; facilitation of catecholamine release is mediated by P2X receptors, whereas inhibition is mediated by the activation of an unidentified P2Y receptor (Von Kügelgen et al., 1989; Boehm and Kubista, 2002). Evidence for inhibitory presynaptic P2Y receptor(s)-regulating release of catecholamine as well as other neurotransmitters in the central nervous system is also accumulating (Cunha and Ribeiro 2000; Zhang et al., 2003). Identifying the nucleotide receptor subtypes that mediate presynaptic inhibition has been compli-

This work was supported by a project grant from the Biotechnology and Biological Sciences Research Council (to S.J.E.), a studentship from the Medical Research Council (to A.D.P.), and a project grant from the Wellcome Trust (to E.P.S.).

S.J.E. and A.D.P. contributed equally to the work.

Article, publication date, and citation information can be found at http://molpharm.aspetjournals.org.
doi:10.1124/mol.104.000224.

ABBREVIATIONS: VOCC, voltage-operated calcium channel; I_{Ca}, calcium current; C_m, membrane capacitance; PPADS, pyridoxal-phosphate-6-azophenyl-2′,4′ disulfonic acid; 2-MeSATP, 2-methylthio-ATP; 2-MeSADP, 2-methylthio-ADP; PTX, pertussis toxin; ARC69931MX, N^6-(2-methylthioethyl)-2-(3,3,3-trifluoropropylthio)-β,γ-dichloromethylene ATP; DMEM, Dulbecco's modified Eagle's medium; PCR, polymerase chain reaction; RACE, rapid amplification of cDNA ends; RT-PCR, reverse transcriptase-polymerase chain reaction; TM, transmembrane; PLC, phospholipase C; ATPγS, adenosine-5′-*O*-(3-thio)triphosphate; BAPTA, 1,2-bis(2-aminophenoxy)ethane-*N*,*N*,*N*′,*N*′-tetraacetic acid.

cated by the inaccessibility of the majority of mammalian nerve terminals, complexity arising from neural circuits in which multiple P2 receptors may be activated, stimulation of P1 adenosine receptors after breakdown of purines by ectonucleotidases, and the limited availability of P2 receptor subtype-selective agonists and antagonists.

Adrenal chromaffin cells are embryonically derived from precursors of sympathetic neurons; they also release catecholamines and ATP by Ca^{2+}-regulated exocytosis and express inhibitory P2 receptors that couple to neuronal VOCCs (Diverse-Pierluissi et al., 1991; Gandia et al., 1993; Currie and Fox, 1996). Moreover, evidence for an autocrine feedback loop similar to that proposed for sympathetic neurons involving an inhibitory P2Y-like receptor has been reported (Carabelli et al., 1998). In a previous study, we used combined C_m measurements and voltage-clamp recordings to examine the mechanisms underlying purinergic inhibition of exocytosis in chromaffin cells (Powell et al., 2000). We showed that the purine analog 2-methylthio-ATP (2-MeSATP) inhibits Ca^{2+} entry through N- and P/Q-type VOCCs and, consequently, stimulus-evoked changes in C_m through a PTX-sensitive G protein. The aim of this study was to expand on this finding by determining the molecular identity of the P2Y receptor(s) involved. Here, we provide evidence for two inhibitory PTX-sensitive $G_{i/o}$-coupled P2Y receptors in bovine chromaffin cells. One of these receptors shows a pharmacology similar but not identical (ATP being a full agonist and equipotent to ADP) with the human $P2Y_{12}$ receptor, whereas the second receptor is UTP-sensitive and hence shows a pharmacology not matching any of the known $G_{i/o}$-coupled P2Y receptors. To confirm the role of $P2Y_{12}$ in VOCC inhibition, we cloned the bovine $P2Y_{12}$ receptor from bovine chromaffin cells and expressed this receptor in *Xenopus laevis* oocytes coexpressing inward-rectifier potassium channels made up of rat Kir3.1 and Kir3.4. The pharmacological properties of this cloned receptor closely mirrored the pharmacology observed in chromaffin cells except that UTP was a very weak partial agonist. We therefore conclude that $P2Y_{12}$ and another yet-unidentified $G_{i/o}$-protein–coupled UTP-sensitive receptor inhibit VOCCs and exocytosis in chromaffin cells. These findings support the view that $G_{i/o}$-coupled P2Y receptors may also act as presynaptic inhibitory receptors in other neuronal systems to regulate neurotransmitter release.

Materials and Methods

Chromaffin Cell Culture. Chromaffin cells were prepared by collagenase digestion of bovine adrenal glands as described previously (Powell et al., 2000). Adrenal glands from 18- to 24-month-old cows were obtained from a local abattoir and were retrogradely perfused at 25 ml/min for 30 min at 37°C with the digestive enzymes collagenase type 2 (0.03%) (Worthington Biochemicals, Freehold, NJ) and DNase I (0.0013%) (Roche Diagnostics, Indianapolis, IN) added to Locke's solution [154.2 mM NaCl, 2.6 mM KCl, 2.2 mM K_2HPO_4, 0.85 mM KH_2PO_4, 10 mM glucose, 5 mM HEPES, and 0.0005% phenol red (Invitrogen, Paisley, UK); pH adjusted to 7.2 with NaOH]. After surgical removal of the cortex, the medulla was dissected, cut into small pieces, placed in a trypsinization flask with fresh enzyme solution, and stirred at slow speed for 30 min at 37°C. Cells were washed twice with Earle's balanced salt solution (Invitrogen) and resuspended in Dulbecco's modified Eagle's medium (DMEM) (Invitrogen) supplemented with 44 mM $NaHCO_3$, 15 mM HEPES, 10% fetal calf serum (Invitrogen), 1% glutamine, 1% penicillin/streptomycin solution, 2.5 mg/ml gentamycin, 0.5 mg/ml 5′-fluorodeoxyuridine, and 0.01 mg/ml cytosine-β-δ-arabino-furanoside. Cells were plated on glass coverslips coated with Matrigel (BD Biosciences Discovery Labware, Bedford, MA) at an approximate density of 800 cells/mm^2. Approximately 80% of the media was replaced 24 h after plating, and cells were maintained for up to 7 days in a humidified atmosphere of 95% O_2/5% CO_2 at 37°C.

$[Ca^{2+}]_i$ Measurements in Bovine Chromaffin Cells. Cells were loaded with the Ca^{2+} indicator Fura 2/acetoxymethyl ester by the addition of 5 μM Fura 2/acetoxymethyl ester (Molecular Probes, Eugene, OR) to DMEM and incubated for 25 min at 37°C. Cells were then washed with fresh DMEM and incubated a further 15 min at 37°C. Isolated fluorescent chromaffin cells were alternately illuminated at 340 and 380 nm using a monochromator (TILL Photonics, Gräfelfing, Germany) controlled by the data acquisition software. Emission >430 nm was collected with a photomultiplier tube (TILL Photonics) and sampled approximately every 12 ms. Data were stored on personal computers, and ratios of 340/380 nm were calculated offline (AxoBASIC-written software; Axon Instruments Inc., Union City, CA).

Electrophysiological Recordings in Bovine Chromaffin Cells. A coverslip carrying chromaffin cells was placed in a microperfusion chamber (~200-μl volume) on the stage of an inverted phase-contrast microscope (Diaphot 200; Nikon, Tokyo, Japan). Cells were continuously superfused with an external solution consisting of 130 mM NaCl, 2 mM KCl, 1 mM $MgCl_2$, 5 mM $CaCl_2$, 10 mM glucose, and 10 mM HEPES adjusted to pH 7.2 with NaOH; osmolarity, ~280 mOsM. Special care was taken to superfuse cells at a high rate (~3 ml/min) throughout the experiment and to select well-isolated single cells for recording to avoid compounding effects of endogenously released modulators (Carabelli et al., 1998). Ionic currents were recorded in whole-cell or perforated patch-clamp configuration using borosilicate glass electrodes coated with Sylgard 184 (Dow Corning, Midland, MI) and fire-polished on a microforge to a resistance of 1 to 2 MΩ. Electrodes were filled with an internal solution consisting of 145 mM cesium-glutamate (Calbiochem, Nottingham, UK), 10 mM HEPES, 9.5 mM NaCl, 0.3 mM BAPTA (Molecular Probes), adjusted to pH 7.2 with CsOH (MP Biomedicals, Irvine, CA); osmolarity, ~280 mOsM. For whole-cell recording experiments, 2 mM Mg-ATP was added to the internal solution to prevent rundown of VOCCs and exocytosis. Gramicidin D (Sigma Chemical, Poole, Dorset, UK) at a final concentration of 9.7 μg/ml was used for perforation. For both whole-cell and perforated-patch recordings, series resistance was less than 12 MΩ and compensated (typically >70%) electronically with the patch-clamp amplifier (Axopatch 200B; Axon Instruments). Voltage protocol generation and data acquisition were performed using custom data acquisition software (kindly provided by Dr. A. P. Fox, University of Chicago) running on a Pentium computer equipped with a Digidata 1200 acquisition board (Axon Instruments). Current traces were low pass-filtered at 5 kHz using the 4-pole Bessel filter of the amplifier and digitized at 10 kHz. Chromaffin cells were voltage-clamped at −90 mV, and C_m was sampled with a resolution of 12 ms using a software-based phase-tracking method as described previously (Fidler and Fernandez, 1989; Powell et al., 2000). Data were stored on the computer hard drive and analyzed offline using custom (AxoBASIC; Axon Instruments) and commercial (Origin; OriginLab Corporation, Northampton, MA) software. All experiments were performed at ambient temperature (21–25°C).

Cloning of the Bovine $P2Y_{12}$ Receptor. The strategy used to clone the bovine $P2Y_{12}$ receptor consisted of three sequential rounds of cloning. First, a conserved central region of the receptor was amplified by polymerase chain reaction (PCR) with degenerate primers (PCR1). Second, 5′- and 3′-rapid amplification of cDNA ends (RACE) primers were designed from the sequence obtained from PCR product 1 and used to amplify the 5′ and 3′ ends of the receptor by 5′- and 3′-RACE, respectively (PCRs 2 and 3). Finally, the sequence obtained from PCR products 2 and 3 was used to design

primers to amplify the full-length receptor from bovine chromaffin cell cDNA by RT-PCR. A proofreading polymerase (Bio-X-Act; Bioline Ltd., London, England) was used for all PCR reactions. Total RNA was prepared from bovine chromaffin cells, and 5 μg was used in a first-strand cDNA reaction using $RoRidT_{(17)}$ primer (Harvey and Darlison, 1991) and Superscript II reverse transcriptase according to the manufacturer's instructions (Amersham Biosciences UK, Ltd., Little Chalfont, Buckinghamshire, UK). The degenerate primers for PCR1, y12degF (5′-TTTCTGTTGYCATCTGGCCMTTCATG-3′) and y12degR (5′-GGTCACCACCWTCYTGTYCTTTYTTC-3′) were designed from homologous regions of the human mouse and rat $P2Y_{12}$ sequences (accession numbers NM_022788, AK013804, and NM_022800, respectively). 5′ RACE (PCR2) was performed using a SMART RACE kit (BD Biosciences Clontech, Palo Alto, CA) according to the manufacturer's instructions with the sequence-specific primer TEW81 (5′-GCCAAACCAGACCAAACTCTGACTTCAG-3′) designed from the sequence of PCR1. 3′ RACE (PCR3) was performed using the primers Ro (Harvey and Darlison, 1991) and bY12RACEfor (5′-GGTGCTGGCAAAGTCCCCAAGAA-3′). The primers 2ndby12fullfor (5′-GACGGAAATACAGTGTCTGC-3′) and 2ndby12fullrev (5′-CTTGCCTTTGGGGAGTT-3′) were designed from the sequence obtained from PCRs 1 and 2 and were used in RT-PCR to amplify the full-length $P2Y_{12}$ receptor from first-strand cDNA prepared from bovine chromaffin cells. PCR products were cloned into the plasmid pCDNA3 (Invitrogen, Carlsbad, CA) and two independent colonies sequenced on both strands (automated ABI sequencing service, Protein and Nucleic Acid Laboratory, University of Leicester, Leicester, UK).

RT-PCR Analysis. RT-PCR was performed on first-strand cDNA prepared from bovine chromaffin cells as described above. The only published bovine P2Y sequence available for primer design was that of $P2Y_1$ (Henderson et al., 1995). BLAST homology searches of the bovine expressed sequence tag database found sequences corresponding to the bovine $P2Y_2$, $P2Y_6$, and $P2Y_{14}$ receptors (accession numbers BM031311, BI680595, and CB429080, respectively), allowing for the presence of transcripts for $P2Y_1$, $P2Y_2$, $P2Y_6$, $P2Y_{12}$, and $P2Y_{14}$ to be analyzed in addition to the published bovine $P2Y_1$ (primer sequences in Table 1).

Electrophysiological Recordings in *X. laevis* Oocytes. *X. laevis* oocytes expressing the rat inwardly rectifying potassium channels Kir 3.1 and Kir 3.4 were used to assess the function of the cloned bovine $P2Y_{12}$ receptor in a system similar to that used by Hollopeter and coworkers (2001) to characterize the human $P2Y_{12}$ receptor. Plasmids for rat Kir 3.1 and Kir 3.4 were a kind gift from Dr. M. Boyett (University of Leeds, Leeds, UK). cRNA was transcribed from linearized $P2Y_{12}$, Kir 3.1, and Kir 3.4 plasmids using the mMessage mMachine system (Ambion, Austin, TX) according to the manufacturer's instructions. Defolliculated stage-V to -VI *X. laevis* oocytes were injected with 1.25 ng of Kir 3.1, 1.25 ng of Kir 3.4, and 50 pg of $P2Y_{12}$ cRNA in a total volume of 50 nl using an INJECT + MATIC microinjector (J. Alejandro Gaby, Geneva). Oocytes were stored at 18°C in ND96 buffer (96 mM NaCl, 2 mM KCl, 1.8 mM $CaCl_2$, 1 mM $MgCl_2$, 5 mM sodium pyruvate, and 5 mM HEPES, pH 7.6) before use 3 to 7 days later.

Two-electrode voltage-clamp recordings were made from oocytes using a Turbo TEC 10C amplifier (NPI Electronic GmbH, Tamm, Germany) with a Digidata 1200 analog-to-digital converter (Axon Instruments) and WinWCP acquisition software (Dr. J. Dempster, University of Strathclyde, Glasgow, Scotland). Agonists and antagonists were bath-perfused using a custom-built rapid-exchange perfusion system. Oocytes were initially perfused with ND96 buffer to obtain a value for the resting membrane potential (typically ~−70 mV for Kir-injected oocytes and ~−20 mV for noninjected or $P2Y_{12}$ only-injected oocytes) before exchange to a solution of 20 mM NaCl, 70 mM KCl, 3 mM $MgCl_2$, and 5 mM HEPES for recording of agonist-evoked membrane currents. Agonist-evoked currents could be measured in oocytes clamped constantly at −60 mV; however, the current required (~5 μA) to clamp at this potential tended to kill cells after ~15 to 30 min. Therefore, to obtain full-concentration response-curve data for individual cells, oocytes were clamped at 0 mV during the initial period of agonist application and in recovery periods between applications. One minute after agonist application commenced, the holding potential was stepped down to −60 mV for 5 s and the peak current was recorded. A ramp from −60 mV to +90 mV over 2 s was applied after the 5-s recording period to visualize the inward rectification from the Kir channels, verifying that the cell was still in a healthy condition. Currents in the presence of agonist were normalized to the mean of recordings taken 5 min before and 5 min after in the absence of agonist.

All drugs were made up as concentrated stock solutions in distilled water and stored in aliquots at −20°C until use. Stocks were thawed once and diluted into the superfusing solution. Nucleotide analogs were obtained from Sigma. 2-MeSATP and pyridoxalphosphate-6-azophenyl-2′,4′-disulfonic acid (PPADS) were obtained from Tocris Cookson Inc.(Bristol, UK). PTX (Sigma) was dissolved in 50% glycerol containing 50 mM Tris, 10 mM glycine, and 0.5 M NaCl, pH 7.5.

Data Analysis. Ca^{2+} entry into chromaffin cells was determined by integration of I_{Ca}. The left limit was set ~3 ms into the voltage pulse to exclude the major portion of the contaminating Na^+ current. ΔC_m measurements were performed as described previously (Powell et al., 2000).

Concentration-response data obtained from individual cells were fitted with the Hill equation $Y = ((X)^{nH} \cdot M)/((X)^{nH} + (EC_{50})^{nH})$, where Y is the response, X is the agonist concentration, n_H is the Hill coefficient, M is maximum response, and EC_{50} is the concentration of agonist evoking 50% of the maximum response. pEC_{50} is the $-\log_{10}$ of the EC_{50} value. Data are presented as mean ± S.E.M., and differences between means were tested using either paired or independent Student's t test, as appropriate.

Results

Measurements of I_{Ca} in Chromaffin Cells. The effects of adenosine and uridine nucleotides on I_{Ca} in bovine chromaffin cells were examined (Fig. 1). Currents were activated every 30 s with step depolarizations to +20 mV from a holding potential of −90 mV. Superfusion with ATP or the P2Y-selective analog 2-MeSATP had no effect on the holding current but reversibly inhibited I_{Ca} by 45 ± 3% (100 μM ATP, n = 13) and 44 ± 4% (100 nM 2-MeSATP, n = 11). UTP (100 μM) also inhibited I_{Ca} (36 ± 6%, n = 11) without changing the holding current. Preceding the test pulse by a 20-ms depolarizing prepulse to 120 mV reduced the inhibitory effect

TABLE 1
Primer sequences used for RT-PCR analysis of P2Y expression in bovine chromaffin cells

Gene	Forward Primer	Reverse Primer	Expected Size
			bp
$P2Y_1$	5′-GCCAGCCCGTTCAAATG-3′	5′-CAGCCCAAAATCAGCACC-3′	599
$P2Y_2$	5′-ACTTCGTCACCACCAGC-3′	5′-GAAAGGCAGAAAGCAGAG-3′	275
$P2Y_6$	5′-CTACTAAGGCGTGCGTTTC-3′	5′-GGGAGCAGGCATACAGC-3′	433
$P2Y_{12}$	5′-TGATCGCTACCAGAAGACCACCAG-3′	5′-TTCATGCCAAACCAGACCAAACTC-3′	205
$P2Y_{14}$	5′-GCATCGTGTTCTTCGGGCTCA-3′	5′-TGTAGGGGATTCTGGCAATGTGGTA-3′	447

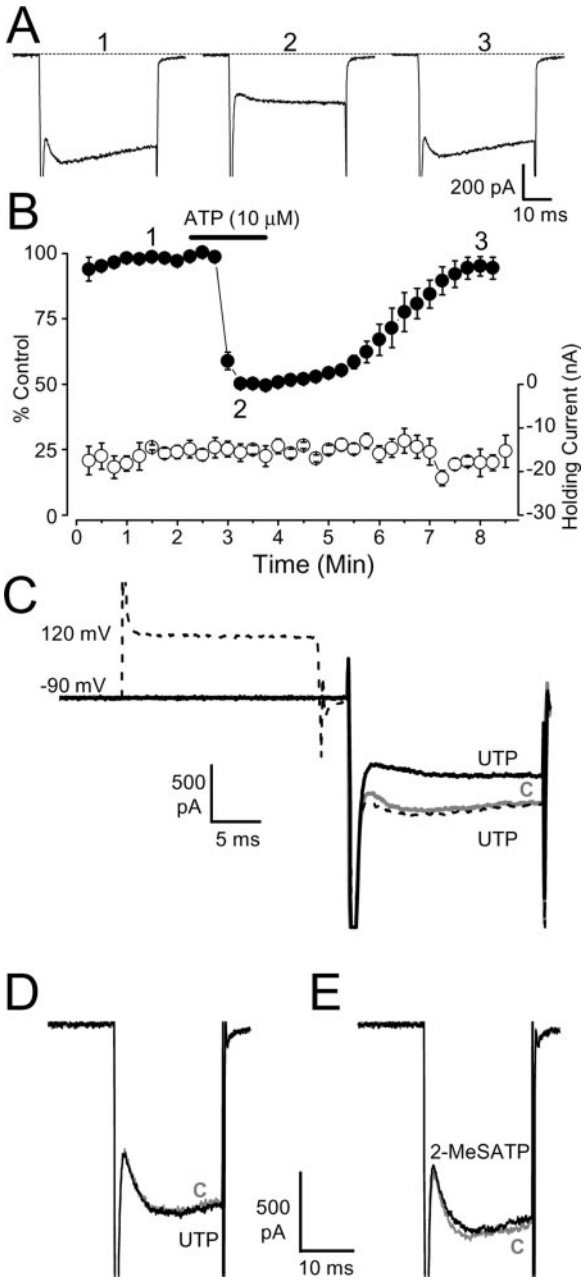

Fig. 1. P2Y inhibition of I_{Ca} in adrenal chromaffin cells. A, representative current traces from a single cell demonstrating ATP (10 μM) inhibition of I_{Ca} evoked by 20-ms voltage steps from −90 mV to a test potential of +20 mV at a frequency of 0.067 Hz. Currents were recorded at the time points illustrated in B. The rapidly inactivating (<3 ms) inward currents seen at the beginning of the traces are caused by opening of tetrodotoxin-sensitive voltage-activated Na^+ channels; these currents have been truncated for illustrative purposes only. B, diary plots of the effect of ATP on normalized Ca^{2+} entry (●) as measured by integrating I_{Ca}, and corresponding holding current (○), measured at −90 mV, 3 ms before application of the voltage step. Data shown are the mean of four cells ± S.E.M. The bar above the graph indicates the time of agonist application. C, superimposed current traces recorded in a single chromaffin cell before (solid gray line) and during (solid black line) application of UTP (100 μM) in response to a 20-ms test pulse from −90 mV to +20 mV. Preceding the test pulse by a 20-ms depolarization to +120 mV (broken line) reversed the inhibition by UTP. D, superimposed current traces from a PTX-treated chromaffin cell before (solid gray line, labeled C) and during application of UTP (100 μM) (solid black line). E, superimposed current traces from another PTX-treated chromaffin cell recorded before (solid gray line, labeled C) and during application of 2-MeSATP (100 nM) (solid black line). PTX treatment completely blocked the inhibitory effects of nucleotides of I_{Ca}.

of 2-MeSATP to 15.5 ± 3.5% (n = 3) and of UTP to 8 ± 2% (n = 3) (Fig. 1C). The voltage-dependence of the inhibitory effect was also observed by examining the effect of 2-MeSATP on the current-voltage relationship (data not shown). Inhibition of I_{Ca} by 2-MeSATP was significantly reduced at potentials positive to +30 mV. Furthermore, 2-MeSATP produced a significant depolarizing shift in the activation curve (V_{50} control, 14.8 ± 3.7 mV; 2-MeSATP, 22.4 ± 4.7 mV; n = 6, $p <$ 0.05). The voltage-sensitivity of the inhibitory effects of the purines and pyrimidines on I_{Ca} is consistent with a signaling pathway that involves direct modulation of the channels by $G_{\beta}\gamma$ subunits (Dolphin, 2003). Treatment of chromaffin cells with PTX (250 ng/ml for 24 h) completely blocked the effect of both 2-MeSATP (3.5 ± 0.8%, n = 4) and UTP (2.8 ± 1.0%, n = 4) (Fig. 1, D and E), confirming the sole involvement of $G_{i/o}$-coupled P2Y receptor(s) in the modulation of I_{Ca}. In contrast to heterologously expressed $P2Y_4$ receptors (Filippov et al., 2003), the inhibition produced by UTP in chromaffin cells was not sensitive to cell dialysis; application of 30 μM UTP (~EC_{50} concentration) inhibited I_{Ca} recorded in the whole-cell configuration by 15.2 ± 2.1% (n = 6) and by 16.3 ± 3.1% (n = 8) in the perforated-patch configuration.

Involvement of Ca^{2+} Mobilizing P2Y or P2X Receptors in VOCC Inhibition. To investigate the possible contribution from Ca^{2+}-mobilizing P2 receptors to inhibition of VOCCs, we loaded chromaffin cells with the Ca^{2+}-sensitive dye Fura 2 to monitor $[Ca^{2+}]_i$. In 10 of 12 cells examined, neither ATP (100 μM) nor UTP (100 μM) produced any increase in $[Ca^{2+}]_i$; in these same cells, histamine (100 μM) and angiotensin II (300 nM), agonists known to activate PLC-coupled receptors in chromaffin cells (Cheek et al., 1993; Teschemacher and Seward, 2000), produced robust increases in $[Ca^{2+}]_i$ (Fig. 2). Superfusion with 2-MeSATP (100 nM) also failed to produce any significant change in basal $[Ca^{2+}]_i$ (n = 4) (also see Fig. 1 in Powell et al., 2000). In 2 of 12 cells, ATP produced a small increase in $[Ca^{2+}]_i$ (mean, 186% of control). However, both of these cells were found to be relatively unresponsive to histamine (mean value of 124% of control compared with 279% for ATP/UTP-nonresponsive cells) and had approximately half the diameter of chromaffin cells usually selected for electrophysiological investigation (mean membrane capacitance, 7.7 ± 0.5 pF, n = 20, corresponding to a diameter of ~15 μm). Whether this minor population of cells corresponds to noradrenergic or cortical cells, which make up 10 to 20% of adrenal medullary cultures, was not investigated further. From these results we can conclude that neither Ca^{2+}-mobilizing P2X receptors nor PLC-coupled $P2Y_1$, $P2Y_2$, $P2Y_4$, and $P2Y_6$ receptors are functionally detectable in the majority of chromaffin cells.

Agonist Profile of P2Y Receptors in Chromaffin Cells. The relative paucity of high-affinity subtype-selective ligands complicates the unambiguous identification of P2Y receptors within intact tissues. The method most commonly used to identify native P2Y receptors is to examine the relative order of potency of numerous purine and pyrimidine analogs. We examined the efficacy of a number of commonly used purine and pyrimidine analogs to inhibit I_{Ca} in chromaffin cells. Agonist-profiling yielded an agonist order of potency of 2-MeSATP ≈ 2MeSADP ≫ ATP ≈ ADP ≥ ATPγS > UTP ≥ UDP (Fig. 3A). $\alpha\beta$-Methylene-ATP and adenosine were inactive (100 μM, data not shown). 2-MeSATP, 2-MeSADP, ATP, ADP, and ATPγS were full agonists

with mean EC_{50} values of 0.49 nM ($n = 4$), 0.73 nM ($n = 4$), 347 nM ($n = 4$), 387 nM ($n = 3$), and 1170 nM ($n = 3$) and Hill slopes of approximately 1 (Table 2).

The uridine nucleotides were less potent than the adenosine analogs (Table 2), and UTP was incapable of exerting a full inhibitory response (Fig. 3A), suggesting that it may act as a partial agonist on a receptor with mixed purine/pyrimidine sensitivity. To test this possibility, the effects of coapplication of a submaximal concentration of UTP (10 μM) with 2-MeSATP (10 pM to 10 nM) were tested. If UTP was acting as a partial agonist at the same receptor population as those activated by 2-MeSATP, coapplication would be expected to cause a rightward shift in the concentration-response curve and a depression of the maximal response. The IC_{50} values for 2-MeSATP alone and in the presence of UTP (10 μM), however, were similar (0.22 and 0.16 nM) (Fig. 3B), and although a slight decrease in the maximal response was observed (2-MeSATP alone, 48 ± 3%, and 2-MeSATP and UTP, 45 ± 6%; $n = 4$), this was not significant ($p = 0.66$).

In response to prolonged activation, many G-protein–coupled receptors undergo desensitization; UTP-preferring $P2Y_4$ receptors can be distinguished from UDP-preferring $P2Y_6$ receptors in that they show rapid desensitization (Brinson and Harden, 2001). Thus, to further characterize the UTP receptor in chromaffin cells, we examined the rate and cross-desensitization of nucleotide inhibition of I_{Ca} (Fig. 4). The general protocol to study desensitization was an initial 3-min application of either 2-MeSATP or UTP, to evaluate the control inhibition. Subsequent to this, either 2-MeSATP or UTP was applied for 15 min and then washed out briefly before 2-MeSATP and UTP were reapplied to check for cross-desensitization. With prolonged superfusion of UTP, the inhibition of I_{Ca} was reduced from 35 ± 9% to 11 ± 6% (Fig. 4A). In the same cells, application of 2-MeSATP inhibited I_{Ca} by 48 ± 6% and 49 ± 6% ($n = 4$) before and after perfusion with UTP, showing that the decline in I_{Ca} inhibition seen during perfusion with UTP was not caused by rundown of the channels but rather desensitization of the receptor. Moreover, because the response to 2-MeSATP was unaffected by desensitization of the UTP response, we can conclude that there is no cross-desensitization of the purine- and pyrimidine-preferring receptors in these cells. The desensitized response of UTP did not recover after an 11-min wash period. In the converse experiment, it was noted that the inhibitory effect of 2-MeSATP on I_{Ca} did not undergo such pronounced desensitization (Fig. 4B). 2-MeSATP maximally inhibited I_{Ca} by 43 ± 3%. During the 15-min superfusion, the mean inhibition was reduced to 29 ± 4% ($n = 4$). The response to a second application of 2-MeSATP after an 11-min wash period

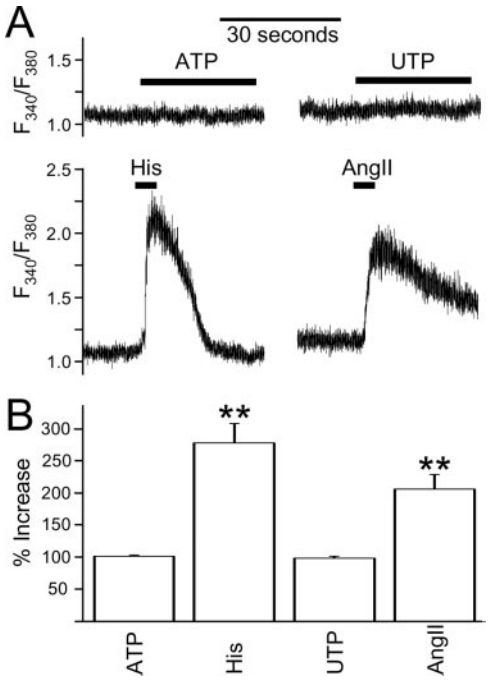

Fig. 2. Involvement of Ca^{2+}-mobilizing P2 receptors. A, representative fluorescence measurements of cytosolic $[Ca^{2+}]_i$. Changes were measured with Fura 2 (expressed as the ratio of emission at 340/380 nm) from a single unclamped chromaffin cell after perfusion with ATP (100 μM), UTP (100 μM), histamine (100 μM), and angiotensin II (300 nM) as indicated by the bars above the trace. B, mean change in resting $[Ca^{2+}]_i$ produced by the indicated agonists for $n = 10$ cells. Neither ATP nor UTP elicits a change in resting $[Ca^{2+}]_i$ in chromaffin cells. **, statistically significant difference ($p < 0.01$) from baseline.

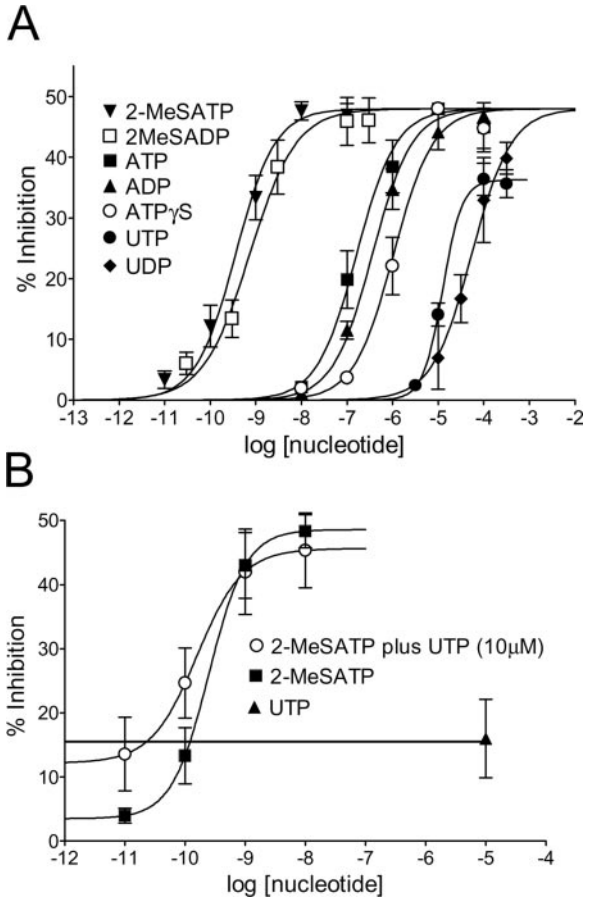

Fig. 3. Concentration-response curves for the inhibition of I_{Ca} by various nucleotides. A, the percentage inhibition in integrated Ca^{2+} entry through I_{Ca} produced by a series of nucleotide agonists is shown. Each agonist concentration was applied for 2 to 3 min until an equilibrium response was observed and then washed for 5 to 10 min to ensure full reversal of the inhibition. All points represent the mean ± S.E.M. of 3 to 15 chromaffin cells. Lines drawn through the data represent the best fit to the Hill equation. B, effect of UTP on the concentration-response curve for 2-MeSATP inhibition of I_{Ca}. Each point represents the mean ± S.E.M. of four cells. UTP (10 μM) was coapplied for 2 min with increasing concentrations of 2-MeSATP (10 pM to 10 nM). UTP did not change the maximum response produced by 2-MeSATP, showing that the responses were nonadditive, nor did it produce a significant shift in the concentration-response curve.

was back to 37 ± 6%. The size of the response to UTP (100 μM) was slightly decreased on the second application (28 ± 13% versus 19 ± 9%; $n = 4$); however, this was not significant.

Antagonist Sensitivity of P2Y Receptors in Chromaffin Cells. The agonist selectivity and PTX sensitivity of the P2Y receptor(s) expressed in bovine adrenal chromaffin cells do not match that reported for any single cloned mammalian P2Y receptor. We therefore proceeded to examine the antagonist selectivity of the receptor(s). PPADS has been shown to be an antagonist at $P2Y_1$, $P2Y_2$, $P2Y_6$, and $P2Y_{13}$ receptors (Marteau et al., 2003) but not at $P2Y_4$ receptors (Boyer et al., 1994; Charlton et al., 1996) or human $P2Y_{12}$ receptors (Takasaki et al., 2001). PPADS antagonized the inhibitory effects of 2-MeSATP (1 nM) and UTP (30 μM) in a reversible manner. Schild analysis of PPADS antagonism of 2-MeSATP inhibition of I_{Ca} showed that the antagonist was acting in a competitive manner, with an apparent pA_2 value of 6.42 ± 0.33 (Fig. 5A). Examination of whether PPADS produced competitive antagonism of the UTP-induced inhibition of I_{Ca} was not carried out because of the low potency of UTP. Finally, we examined the ability of the antithrombotic drug ARC69931MX, reported to be selective for $P2Y_{12}$ and $P2Y_{13}$ receptors (Ingall et al., 1999; Marteau et al., 2003), to antagonize the regulation of I_{Ca} in chromaffin cells. Superfusion with ARC69931MX (1 μM) for 1 to 3 min had no effect on I_{Ca} (106 ± 12% of control, $n = 4$), but in the same cells it largely abolished the inhibition produced by ATP (100 μM) from 49 ± 4% to 6 ± 5% ($n = 4$). Schild analysis of ARC69931MX antagonism of 2-MeSADP inhibition of I_{Ca} gave an apparent pA_2 value of 9.90 ± 0.06. Inhibition of I_{Ca} by 30 μM UTP, however, persisted in the presence of ARC69931MX (mean, 20 ± 9%; $n = 3$), supporting the notion that distinct ATP and UTP receptors are expressed by chromaffin cells.

Measurements of Exocytosis in Chromaffin Cells. An increase in C_m follows vesicle fusion after Ca^{2+} entry and provides a measurement of exocytosis corresponding to 2 fF per vesicle fusion. We therefore used C_m measurements to determine the effects of VOCC inhibition by nucleotides on exocytosis from bovine chromaffin cells (Fig. 5, B and C). Application of ATP (100 μM) resulted in a marked decrease in vesicle fusion (Fig. 5B). This inhibitory effect of ATP on exocytosis was completely blocked by the $P2Y_{12}$-specific antagonist ARC69931MX (Fig. 5C).

Cloning of the Bovine $P2Y_{12}$ Receptor. Taken together, the pharmacological data obtained from bovine chromaffin cells suggest that the purine receptor responsible for inhibition of I_{Ca} and exocytosis is most similar to that of $P2Y_{12}$ or $P2Y_{13}$ except that ATP was a full agonist rather than a weak partial agonist (Marteau et al., 2003) and PPADS is an antagonist. Unlike the pharmacology of the nucleotide responses observed in the P2Y receptors expressed in bovine chromaffin cells, human $P2Y_{13}$ is unresponsive to both 2-MeSATP and ATP (Communi et al., 2001). Human $P2Y_{12}$, however, is responsive to 2-MeSATP in the nanomolar range and ATP in the micromolar range (Takasaki et al., 2001). We therefore cloned the bovine $P2Y_{12}$ receptor to compare its pharmacology with the purine-sensitive $G_{i/o}$-coupled P2Y receptor expressed in bovine chromaffin cells. A PCR product of 1145 base pairs was amplified from bovine chromaffin cell cDNA using the primers 2ndby12fullfor and 2ndby12fullrev. This sequence is available in the European Molecular Biology Laboratory database under the accession number AJ623293. The sequence contained an open-reading frame of 339 amino acids with a consensus Kozak sequence at the starting methionine. CLUSTAL alignment of the deduced bovine $P2Y_{12}$ amino acid sequence with human, rat, and mouse P2Y receptors confirmed that this sequence corresponds to $P2Y_{12}$ and not to a related receptor such as $P2Y_{13}$ or $P2Y_{14}$ (Fig. 6A). The cloned bovine receptor showed strong sequence identity to the known mammalian $P2Y_{12}$ sequences with percentage identities of 89.4, 84.4, and 85.9% for human, rat, and mouse $P2Y_{12}$ sequences, respectively. Alignment of the human and bovine $P2Y_{12}$ amino acid sequences (Fig. 6B) demonstrates the positions of the 37 residues that differ between species. There are no differences in amino acid sequence in the region from TM6 through to TM7, a region that has been implicated previously in agonist binding in the $P2Y_2$ receptor (Erb et al., 1995).

Measurements of Potassium Currents in *X. laevis* Oocytes Expressing the Bovine $P2Y_{12}$ Receptor. Coexpression in *X. laevis* oocytes of the cloned cardiac inward-rectifier subunits Kir 3.1 and Kir 3.4 resulted in robust expression of an inwardly rectifying potassium channel (Fig.

TABLE 2
Pharmacological data for endogenous receptors in bovine chromaffin cells and the cloned bovine $P2Y_{12}$ receptor expressed in *X. laevis* oocytes
Values are presented as mean ± S.E.

	EC_{50}	pEC_{50}	Hill Slope
Chromaffin cells			
2-MeSADP	0.73 nM	9.14 ± 0.10	0.85 ± 0.14
2-MeSATP	0.49 nM	9.45 ± 0.22	1.13 ± 0.16
ATP	0.35 μM	6.67 ± 0.25	1.24 ± 0.30
ADP	0.39 μM	6.44 ± 0.12	0.93 ± 0.08
UDP	34.86 μM	4.48 ± 0.09	1.53 ± 0.35
UTP	14.24 μM	4.89 ± 0.11	1.92 ± 0.44
ATPγS	1.17 μM	5.99 ± 0.16	1.38 ± 0.13
Oocytes			
2-MeSADP	0.28 nM	9.55 ± 0.10	0.63 ± 0.06
2-MeSATP	0.84 nM	9.31 ± 0.21	0.66 ± 0.06
ATP	3.74 μM	5.47 ± 0.10	0.87 ± 0.04
ADP	1.56 μM	5.97 ± 0.17	0.86 ± 0.11
UDP	105.5 μM	4.12 ± 0.64	0.91 ± 0.54
UTP[a]	50.12 μM	4.30 ± 0.40	

[a] Weak partial agonist.
EC_{50}, concentration of nucleotide required to elicit half the maximal response; pEC_{50}, −log10 EC_{50} (molar); Hill slope, gradient of concentration response.

7A). Activation of this channel by $G_{\beta}\gamma$ release was used to characterize the pharmacology of the cloned bovine P2Y$_{12}$ receptor. To confirm the absence of endogenous oocyte channels or receptors that could interfere with results by coupling to the exogenous bovine P2Y$_{12}$ receptor or rat Kir channels, noninjected oocytes, and oocytes injected with cRNA for the bovine P2Y$_{12}$ receptor only or only the Kir 3.1 and Kir 3.4 cRNAs were tested. These oocytes showed no nucleotide-evoked currents (data not shown). When oocytes were coinjected with cRNAs for the bovine P2Y$_{12}$ receptor (50 pg) and rat Kir 3.1 + 3.4 channels (1.25 ng each), nucleotide-evoked currents were observed. These currents reached a peak within 30 s, did not desensitize with the continued agonist application, and decayed back to baseline within 3 min of agonist removal.

Concentration-response data were obtained by using the voltage protocol depicted in Fig. 7A (and described in detail under *Materials and Methods*). Similar to the agonist profile obtained in bovine chromaffin cells, ATP and ADP were essentially equipotent at the cloned bovine P2Y$_{12}$ receptor, showing EC_{50} values of 3.74 μM (pEC_{50} = 5.47 ± 0.10) and 1.56 μM (pEC_{50} = 5.97 ± 0.17), respectively (Fig. 7B). 2-MeSADP and 2-MeSATP were considerably more potent, with EC_{50} values of 0.28 nM (pEC_{50} = 9.55 ± 0.10) and 0.84 nM (pEC_{50} = 9.31 ± 0.21), respectively. Uridine nucleotides showed varying degrees of potency with UDP, a full agonist (EC_{50} = 105.5 μM, pEC_{50} = 4.12 ± 0.64), UTP, a very weak partial agonist (~10% maximal UDP response with 10 mM UTP), and UMP, inactive.

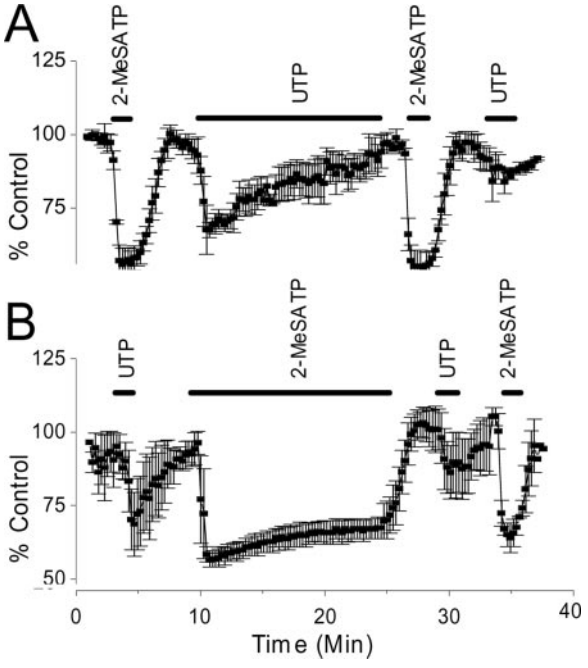

Fig. 4. Inhibition of VOCCs by 2-MeSATP and UTP differ in their desensitization characteristics. VOCCs were evoked at a frequency of 0.067 Hz by a 20-ms depolarization from −90 mV to +20 mV. Data shown are the means of three separate experiments. A, 2-MeSATP (100 nM) was applied for 2 min and then washed out. UTP (100 μM) was then continuously applied for 15 min to induce desensitization of the response. At the end of the 15-min desensitization period, 2-MeSATP was reapplied for a further 2 min to examine whether cross-desensitization had occurred. A further UTP application followed to determine recovery from desensitization. B, converse experiment in which the order of agonist applications was switched, as indicated.

The effects of the antagonists ARC69931MX and PPADS were also determined at the cloned P2Y$_{12}$ receptor in *X. laevis* oocytes (Fig. 7C). The P2Y$_{12}$-specific antagonist

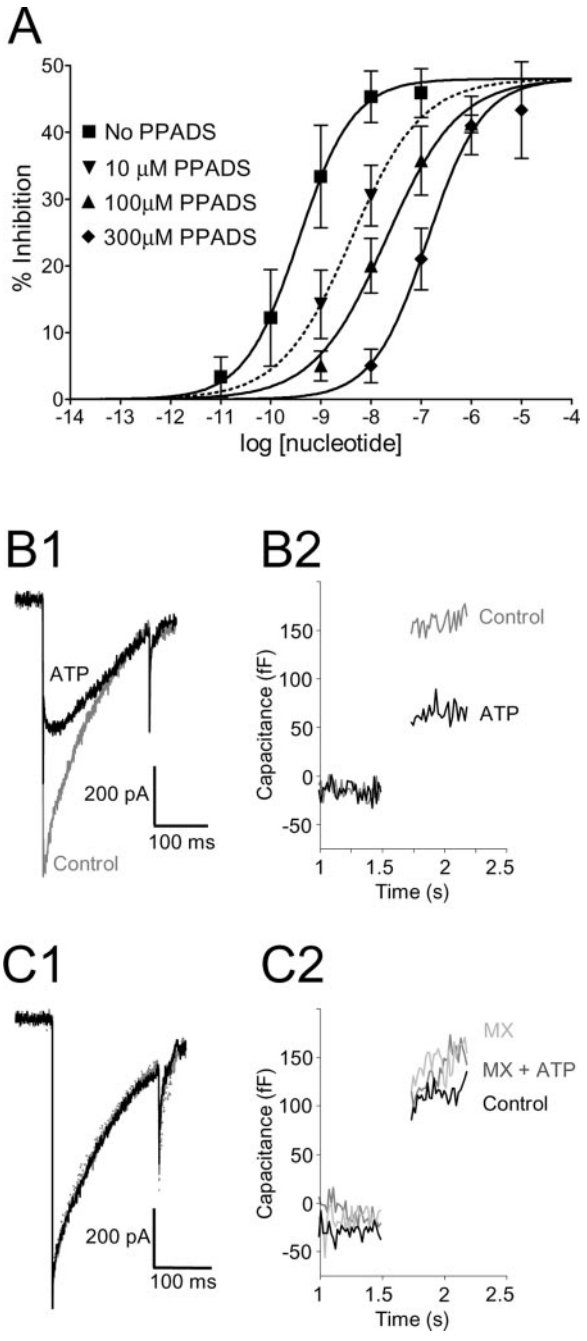

Fig. 5. P2Y$_{12}$ inhibition of VOCCs and exocytosis. A, concentration-response curves for the inhibition of I_{Ca} in chromaffin cells exposed to 2-MeSATP in the absence or presence of PPADS. Data in the presence of 10 μM PPADS were constrained to a Hill slope of 1 and minimum and maximum values of 0 and 48%, respectively (broken line). Schild regression analysis of the data (not shown) yielded a pA_2 value of 6.42 ± 0.34. Data illustrated are the means ± S.E.M. of three such experiments. B1 and C1, superimposed Ca^{2+}-current traces recorded in a single chromaffin cell held at −90 mV and stepped for 200 ms to +20 mV before (solid gray line) and during superfusion with 100 μM ATP (solid black line), in the absence (B1, control) or presence (C1) of 1 μM ARC69931MX. B2 and C2, corresponding ΔC_m recorded in response to currents shown in B1 and C1. Gaps in the C_m traces represent when a voltage step was applied; the increases in C_m that follow Ca^{2+} entry provide a measure of exocytosis corresponding to 2 fF per vesicle fusion.

ARC69931MX completely blocked responses of the bovine $P2Y_{12}$ receptor to 10 μM ADP (IC_{50} = 0.78 nM, pIC_{50} = 8.67 ± 0.06) and 10 μM ATP (IC_{50} = 2.1 nM, pIC_{50} = 9.14 ± 0.44). Furthermore, the responses to 1 mM UDP, a concentration normally eliciting a 100% response, was blocked completely by 1 μM ARC69931MX (n = 4 oocytes) (data not shown). PPADS, a nonspecific P2 receptor antagonist, blocked responses to 1 nM 2MeSATP with an IC_{50} value of 1.71 μM (pIC_{50} = 5.80 ± 0.05).

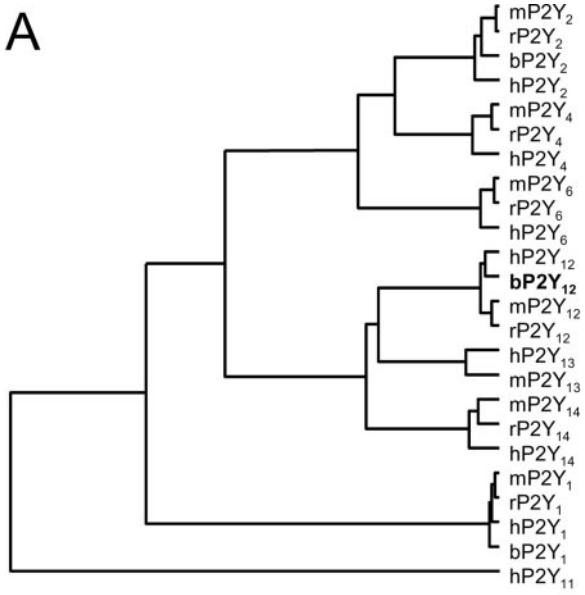

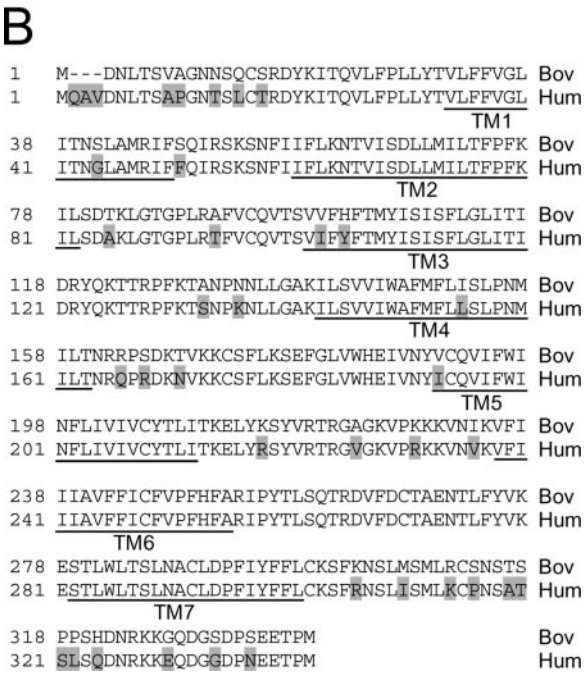

Fig. 6. Bovine $P2Y_{12}$ sequence analysis. A, phylogenetic analysis of bovine $P2Y_{12}$. P2Y amino acid sequences available for human (h), mouse (m), rat (r), and bovine (b) were aligned using the program CLUSTAL. Accession numbers for the sequences used in the alignment are as follows: $mP2Y_2$, P35383; $rP2Y_2$, P41232; $bP2Y_2$, O18951; $hP2Y_2$, P41231; $mP2Y_4$, Q9JJS7; $rP2Y_4$, O35811; $hP2Y_4$, P51582; $mP2Y_6$, Q9ERK9; $rP2Y_6$, Q63371; $hP2Y_6$, Q15077; $hP2Y_{12}$, Q9H244; $bP2Y_{12}$, AJ623293; $mP2Y_{12}$, Q9CPV9; $rP2Y_{12}$, Q9EPX4; $hP2Y_{13}$, Q9BPV8; $mP2Y_{13}$, NP_083084; $mP2Y_{14}$, Q9ESG6; $rP2Y_{14}$, O35881; $hP2Y_{14}$, Q15391; $mP2Y_1$, P49650; $rP2Y_1$, P49651; $hP2Y_1$, P47900; $bP2Y_1$, P48042; and $hP2Y_{11}$, Q96G91. B, alignment of the human (Hum) and bovine (Bov) $P2Y_{12}$ amino acid sequences. Residues differing between the two sequences are shaded in the human sequence. Transmembrane domains 1 to 7 are indicated as lines.

Detection of P2Y Receptor mRNA in Bovine Chromaffin Cells by RT-PCR. Of the nine known mammalian P2Y receptors ($P2Y_1$, $P2Y_2$, $P2Y_4$, $P2Y_6$, $P2Y_{11}$, $P2Y_{12}$, $P2Y_{13}$, $P2Y_{14}$, and $P2Y_{15}$) it was possible to design sequence-specific primers for bovine $P2Y_1$, $P2Y_2$, $P2Y_6$, $P2Y_{12}$, and $P2Y_{14}$ (Table 1). Amplicons of the expected size were obtained for all primer pairs when PCR was performed on bovine genomic DNA (data not shown). Three primer pairs ($P2Y_1$, $P2Y_{12}$, and $P2Y_{14}$) gave amplicons of the expected size when RT-PCR was performed on first-strand cDNA prepared from isolated bovine chromaffin cells (Fig. 8). Faint bands were observed in amplifications using $P2Y_2$ and $P2Y_6$ primers. However, these bands were not of the correct size and are therefore likely to correspond to nonspecific amplifications. No bands were observed in control reactions minus reverse transcriptase, confirming the absence of contaminating genomic DNA. Thus, from the RT-PCR analysis, transcripts for $P2Y_1$, $P2Y_{12}$, and $P2Y_{14}$ but not $P2Y_2$ or $P2Y_6$ could be detected in bovine chromaffin cells.

Discussion

Like other classical neurotransmitters, it is now clear that postsynaptic receptors for nucleotides exist as either ligand-gated ion channels (ATP-sensitive P2X receptors), ideally suited to rapid neurotransmission, or G-protein–coupled P2Y receptors, suited to slower modulatory roles. Evidence for presynaptic nucleotide receptors in the peripheral and central nervous systems is also accumulating (Cunha and Ribeiro, 2000; Boehm and Kubista, 2002; Zhang et al., 2003). However, positive identification of the receptor subtypes mediating presynaptic effects of nucleotides has been complicated by a lack of selective pharmacological tools and a paucity of data from receptor knockout studies. We have shown previously that activation of a PTX-sensitive $G_{i/o}$-protein–coupled P2Y receptor in adrenal chromaffin cells inhibits exocytosis and Ca^{2+} entry through N-type and P/Q-type VOCCs (Powell et al., 2000); a similar mechanism is believed to underlie purinergic presynaptic inhibition of sympathetic neurotransmission. In this study, we have identified one of the inhibitory receptors in chromaffin cells as $P2Y_{12}$. In addition, we have found evidence for a second UTP-preferring receptor that acts in a similar manner. The modulation of VOCCs in chromaffin cells by both nucleotide receptors showed all the characteristic properties of $G_{i/o}$ signaling, namely sensitivity to voltage and PTX (Dolphin, 2003). This signaling pathway is known to be membrane-delimited, to be independent of diffusible second messengers, and to involve direct coupling between the receptor, $G_{i/o}$ $\beta\gamma$ subunits, and intracellular domains found on the α1A and α1B pore-forming subunits that make up neuronal N- and P/Q-VOCCs.

Similar inhibition of N-type VOCCs by heterologously expressed $P2Y_{12}$ and the closely related $P2Y_{13}$ receptor also has been reported (Simon et al., 2002; Kubista et al., 2003; Wirkner et al., 2004). In the chromaffin-like pheochromocytoma (PC-12) cell line, inhibition of N-type channels by a $P2Y_{12}$-like receptor is found at the cell soma (Vartian and Boehm, 2001; Kubista et al., 2003) as well as in processes

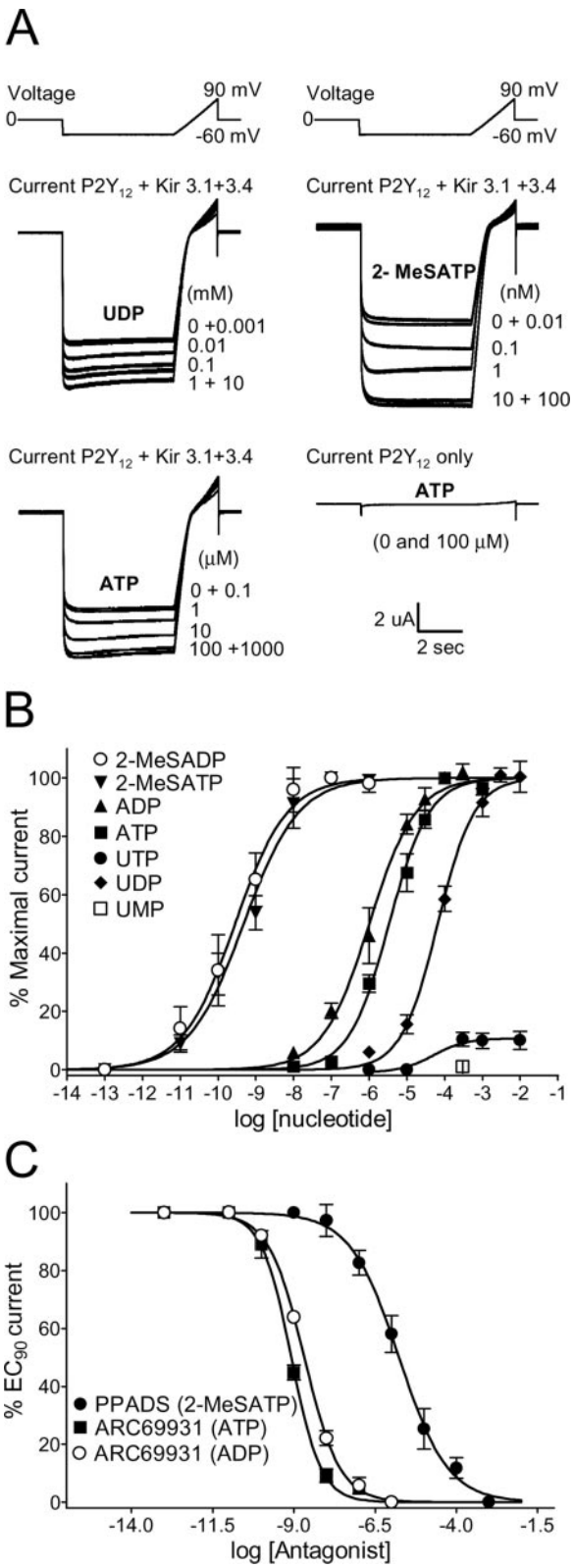

Fig. 7. Concentration-response data for the bovine P2Y$_{12}$ receptor coexpressed with rat Kir 3.1 and Kir 3.4 channels in *X. laevis* oocytes. Two-electrode voltage-clamp recordings were made from oocytes expressing bovine P2Y$_{12}$, rat Kir 3.1, and rat Kir 3.4. A, currents recorded in response to UDP, 2-MeSATP, and ATP. Oocytes were clamped at 0 mV during the initial agonist application and recovery periods between applications. One minute after agonist application commenced, the holding potential was stepped down to −60 mV for 5 s and the peak current was recorded. A ramp from −60 mV to +90 mV over 2 s was applied after the 5-s recording period. No agonist-induced currents or rectification was observed in oocytes expressing bovine P2Y$_{12}$ alone. B, concentration-response curves for the bovine P2Y$_{12}$ receptor expressed in *X. laevis* oocytes coexpressing the rat Kir 3.1 and Kir3.4 channels. Mean currents were normalized to 100 μM ADP (maximal response). Error bars show ± standard error; n = 5 to 6 oocytes. C, the sensitivity of bovine P2Y$_{12}$ to the antagonists PPADS and ARC69931MX was determined in *X. laevis* oocytes coexpressing the rat Kir3.1 and Kir 3.1 channels. Recordings were made at a holding membrane potential of −60 mV using the protocol depicted in A. Currents in response to an EC$_{90}$ application of agonist (10 μM for ADP and ATP; 1 nM for 2-MeSATP) were recorded in the presence of varying concentrations of antagonists and are expressed as a percentage of the EC$_{90}$ response obtained in the absence of antagonist. The P2Y$_{12}$-specific antagonist ARC69931MX completely blocked responses of the bovine P2Y$_{12}$ receptor to 10 μM ADP and 10 μM ATP with IC$_{50}$ values of 0.78 nM (pIC$_{50}$ = 8.67 ± 0.06) and 2.1 nM (pIC$_{50}$ = 9.14 ± 0.44), respectively. PPADS, a nonspecific P2 receptor antagonist, blocked responses to 1 nM 2-MeSATP with an IC$_{50}$ of 1.71 μM (pIC$_{50}$ = 5.80 ± 0.05); n = 4 to 5 oocytes.

(Kulick and von Kügelgen, 2002) in which it contributes to an autocrine-paracrine inhibitory loop regulating exocytotic nucleotide release (Moskvina et al., 2003). One notable difference between the PC-12 receptor and bovine P2Y$_{12}$ receptor is sensitivity to PPADS. We found it to be a competitive antagonist of the bovine receptor, whereas in PC-12 cells, which are rat-derived, it is reported to be ineffective (Vartian and Boehm, 2001; Kulick and von Kügelgen, 2002; Unterberger et al., 2002). Species differences in the pharmacology of other P2Y receptor subtypes have been reported previously (Sak and Webb, 2002).

In this study, we describe the cloning and characterization of a new member of the mammalian P2Y receptor family: bovine P2Y$_{12}$. At the amino acid level, the bovine receptor is similar to human P2Y$_{12}$, with 89% of residues identical between species (compared with 85% between human and rat P2Y$_{12}$). However, the agonist selectivity of the receptor showed some slight differences from that reported for the human P2Y$_{12}$ receptor, most notably for ATP and UDP. Whether ATP acts as an agonist at human P2Y$_{12}$ is unclear and most likely depends on cell type and receptor density. At purified and reconstituted human P2Y$_{12}$, in which nucleotide breakdown has been eliminated, ATP is not an agonist but is rather a low-affinity antagonist (Bodor et al., 2003). However, recombinant human P2Y$_{12}$ expressed in Chinese hamster ovary cells shows an EC$_{50}$ value for ATP (~1 μM) similar to that reported for native rat P2Y$_{12}$ in brain endothelial ,capillary cells (Simon et al., 2002) and to values reported here for bovine P2Y$_{12}$ in chromaffin cells and oocytes. In those studies in which ATP was reported as a P2Y$_{12}$ agonist, ATP potency is an order of magnitude lower than ADP (Simon et al., 2002). At bovine P2Y$_{12}$, however, in both native bovine chromaffin cells and *X. laevis* oocytes coexpressing recombinant bovine P2Y$_{12}$ with rat inwardly rectifying potassium channels, ATP acts as a full agonist equipotent to ADP. Nucleotide breakdown of ATP to ADP can be excluded as an explanation of the bovine P2Y$_{12}$ ATP response, because for this to be the case, it would require that 100% of ATP be instantaneously broken down by *X. laevis* oocytes and bovine chromaffin cells in a constant perfusion system, and in any case, in the bovine chromaffin cell system, ATP was actually slightly more potent than ADP.

A second difference in agonist selectivity between bovine and human P2Y$_{12}$ was the sensitivity to UDP. UDP is inactive at human P2Y$_{12}$ (Hollopeter et al., 2001; Takasaki et al.,

2001). However, at bovine $P2Y_{12}$ expressed in *X. laevis* oocytes, UDP is a full agonist, albeit with a low potency (EC_{50} ~100 μM). Although unlikely, a contamination of the commercial UDP stocks used in this study with 1% ADP or ATP would be enough to explain the UDP sensitivity observed. To rule out this possibility, we performed high-performance liquid chromatography on UDP alone and on UDP spiked with ATP and ADP. No contaminating peak in the sample was greater than 0.01%, and no contaminating peak corresponded to either ATP or ADP. We also observed a small response to UTP in bovine $P2Y_{12}$ expressed in *X. laevis* oocytes (~10% maximal response to 10 mM UTP). At such high concentrations of UTP, the possibility that responses were caused by a breakdown of UTP to UDP could not be ruled out.

The UTP receptor inhibiting I_{Ca} and exocytosis in chromaffin cells has not been identified at the molecular level. UTP does not seem to be acting as a partial agonist at the bovine $P2Y_{12}$ receptor because it was insensitive to ARC69931MX, caused no shift in the 2-MeSATP concentration-response curve, showed no cross-desensitization with the purine receptor in chromaffin cells, and had a very low potency at the cloned receptor. Heterologously expressed $P2Y_2$, $P2Y_4$, and $P2Y_6$ receptors have also been shown to inhibit I_{Ca} in a neuronal expression system (Filippov et al., 1999, 2003). However, there are notable differences between the results from the expression studies and those found with the endogenous receptor in chromaffin cells; thus, even when overexpressed in neurons, $P2Y_2$, $P2Y_4$, and $P2Y_6$ maintain their ability to couple to PTX-insensitive G_q proteins and inhibit M potassium currents, which would lead to an increase in $[Ca^{2+}]_i$. UTP does not cause calcium mobilization or entry in chromaffin cells, indicating that it is not acting through a G_q- or PLC-coupled receptor in these cells. Furthermore, inhibition of I_{Ca} by heterologously expressed $P2Y_4$ is lost in whole-cell recording of neurons, whereas the receptor in chromaffin cells showed no such sensitivity to intracellular dialysis. Because a positive RT-PCR result was obtained for $P2Y_{14}$ expression in bovine chromaffin cells (Fig. 8), we considered the possibility that UTP could be acting as a low-potency agonist at the bovine $P2Y_{14}$ receptor in chromaffin cells.

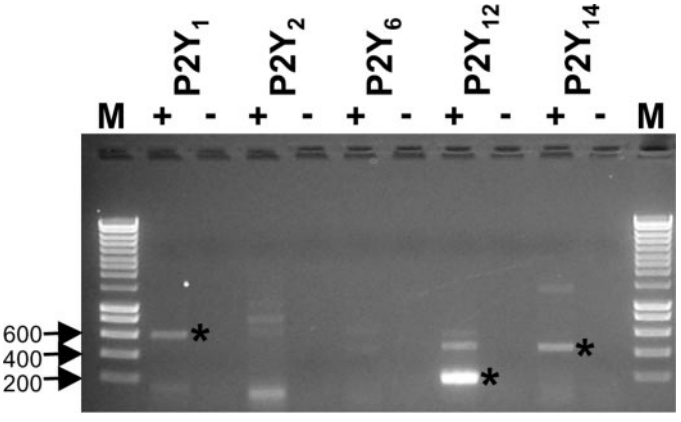

Fig. 8. RT-PCR analysis of total RNA-isolated bovine chromaffin cells. Primers used corresponded to the bovine $P2Y_1$, $P2Y_2$, $P2Y_6$, $P2Y_{12}$, and $P2Y_{14}$ and are detailed in Table 1. Control reactions without reverse transcriptase (−) were run alongside cDNA templates (+) to verify that amplification was not from genomic DNA. ⋆, positive bands of the expected size were observed for $P2Y_1$, $P2Y_{12}$, and $P2Y_{14}$. M, molecular size marker (size in base pairs).

However, UDP-glucose, the cognate ligand for human $P2Y_{14}$, gave no response when tested in bovine chromaffin cells (E. Seward, unpublished data). Thus, either bovine $P2Y_{14}$ does not couple to VOCCs in bovine chromaffin cells or the $P2Y_{14}$ RT-PCR product originated from nontranslated mRNA in chromaffin cells or from $P2Y_{14}$ in a contaminating cell type. It is interesting to note that UTP inhibition of VOCCs has been observed in parasympathetic neurons (Abe et al., 2003), and evidence for a presynaptic inhibitory UTP receptor on sympathetic nerves of the rat and mouse vas deferens has also been reported (Von Kügelgen et al., 1989; Forsyth et al., 1991). Further studies will be required to determine whether one of the still-orphaned G-protein–coupled receptors that share significant sequence identity with the $P2Y_{12}$ receptor represent a pyrimidine-selective $G_{i/o}$-coupled P2Y receptor in the ever-growing P2 receptor family.

Finally, the results from this study confirm that $P2Y_{12}$ receptors, the targets of antithrombotic agents, are not restricted to platelets but are also expressed in neuroendocrine cells, in which they act as inhibitory receptors to regulate the activity of neuronal VOCCs and vesicular neurotransmitter release. Expression of these receptors at nerve terminals could serve as an important autocrine inhibitory feedback loop to regulate neurotransmission in the periphery and mediate heterosynaptic suppression in the central nervous system.

Acknowledgments

We thank Dr. Tania Webb for help and advice with the cloning the bovine $P2Y_{12}$ receptor and preparation of the manuscript, Prof. Mark Boyett for providing the Kir 3.1 and Kir 3.4 plasmids, Prof. Mike Boarder for help with high-performance liquid chromatography analysis of nucleotides, Prof. Alan North for critical review of the manuscript, and AstraZeneca for the kind donation of ARC69931MX.

References

Abbracchio MP, Boeynaems JM, Barnard EA, Boyer JL, Kennedy C, Miras-Portugal MT, King BF, Gachet C, Jacobson KA, Weisman GA, et al. (2003) Characterization of the UDP-glucose receptor (re-named here the $P2Y_{14}$ receptor) adds diversity to the P2Y receptor family. *Trends Pharmacol Sci* **24:**52–55.

Abe M, Endoh T, and Suzuki T (2003) Extracellular ATP-induced calcium channel inhibition mediated by P1/P2Y purinoceptors in hamster submandibular ganglion neurons. *Br J Pharmacol* **138:**1535–1543.

Bodor ET, Waldo GL, Hooks SB, Corbitt J, Boyer JL, and Harden TK (2003) Purification and functional reconstitution of the human $P2Y_{12}$ receptor. *Mol Pharmacol* **64:**1210–1216.

Boehm S and Kubista H (2002) Fine tuning of sympathetic transmitter release via ionotropic and metabotropic presynaptic receptors. *Pharmacol Rev* **54:**43–99.

Boyer JL, Zohn IE, Jacobson KA, and Harden TK (1994) Differential effects of P2-purinoceptor antagonists on phospholipase C- and adenylyl cyclase-coupled P2Y-purinoceptors. *Br J Pharmacol* **113:**614–620.

Brinson AE and Harden TK (2001) Differential regulation of the uridine nucleotide-activated $P2Y_4$ and $P2Y_6$ receptors. *J Biol Chem* **276:**11939–11948.

Carabelli V, Carra I, and Carbone E (1998) Localized secretion of ATP and opioids revealed through single Ca^{2+} channel modulation in bovine chromaffin cells. *Neuron* **20:**1255–1268.

Charlton SJ, Brown CA, Weisman GA, Turner JT, Erb L, and Boarder MR (1996) Cloned and transfected $P2Y_4$ receptors: characterization of a suramin and PPADS-insensitive response to UTP. *Br J Pharmacol* **119:**1301–1303.

Cheek TR, Morgan A, O'Sullivan AJ, Moreton RB, Berridge MJ, and Burgoyne RD (1993) Spatial localization of agonist-induced Ca^{2+} entry in bovine adrenal chromaffin cells: different patterns induced by histamine and angiotensin II and relationship to catecholamine release. *J Cell Sci* **105:**913–921.

Communi D, Gonzalez NS, Detheux M, Brezillon S, Lannoy V, Parmentier M, and Boeynaems JM (2001) Identification of a novel human ADP receptor coupled to G_i. *J Biol Chem* **276:**41479–41485.

Cunha RA and Ribeiro JA (2000) ATP as a presynaptic modulator. *Life Sci* **68:**119–137.

Currie KP and Fox AP (1996) ATP serves as a negative feedback inhibitor of voltage-gated Ca^{2+} channel currents in cultured bovine adrenal chromaffin cells. *Neuron* **16:**1027–1036.

Diverse-Pierluissi M, Dunlap K, and Westhead EW (1991) Multiple actions of extracellular ATP on calcium currents in cultured bovine chromaffin cells. *Proc Natl Acad Sci USA* **88:**1261–1265.

Dolphin AC (2003) G protein modulation of voltage-gated calcium channels. *Pharmacol Rev* **55:**607–627.
Erb L, Garrad R, Wang Y, Quinn T, Turner JT, and Weisman GA (1995) Site-directed mutagenesis of P2U purinoceptors. Positively charged amino acids in transmembrane helices 6 and 7 affect agonist potency and specificity. *J Biol Chem* **270:**4185–4188.
Fidler N and Fernandez JM (1989) Phase tracking: an improved phase detection technique for cell membrane capacitance measurements. *Biophys J* **56:**1153–1162.
Filippov AK, Simon J, Barnard EA, and Brown DA (2003) Coupling of the nucleotide $P2Y_4$ receptor to neuronal ion channels. *Br J Pharmacol* **138:**400–406.
Filippov AK, Webb TE, Barnard EA, and Brown DA (1999) Dual coupling of heterologously-expressed rat $P2Y_6$ nucleotide receptors to N-type Ca^{2+} and M-type K^+ currents in rat sympathetic neurones. *Br J Pharmacol* **126:**1009–1017.
Forsyth KM, Bjur RA, and Westfall DP (1991) Nucleotide modulation of norepinephrine release from sympathetic nerves in the rat *vas deferens*. *J Pharmacol Exp Ther* **256:**821–826.
Gandia L, Garcia AG, and Morad M (1993) ATP modulation of calcium channels in chromaffin cells. *J Physiol* **470:**55–72.
Harvey RJ and Darlison MG (1991) Random-primed cDNA synthesis facilitates the isolation of multiple 5′-cDNA ends by RACE. *Nucleic Acids Res* **19:**4002.
Henderson DJ, Elliot DG, Smith GM, Webb TE, and Dainty IA (1995) Cloning and characterisation of a bovine P2Y receptor. *Biochem Biophys Res Commun* **212:**648–656.
Hollopeter G, Jantzen HM, Vincent D, Li G, England L, Ramakrishnan V, Yang RB, Nurden P, Nurden A, Julius D, et al. (2001) Identification of the platelet ADP receptor targeted by antithrombotic drugs. *Nature (Lond)* **409:**202–207.
Inbe H, Watanabe S, Miyawaki M, Tanabe E, and Encinas JA (2004) Identification and characterization of a cell-surface receptor, $P2Y_{15}$, for AMP and adenosine. *J Biol Chem* **279:**19790–19799.
Ingall AH, Dixon J, Bailey A, Coombs ME, Cox D, McInally JI, Hunt SF, Kindon ND, Teobald BJ, Willis PA, et al. (1999) Antagonists of the platelet P2T receptor: a novel approach to antithrombotic therapy. *J Med Chem* **42:**213–220.
Kubista H., Lechner S, and Boehm S (2003) Attenuation of the P2Y receptor-mediated control of neuronal Ca^{2+} channels by antithrombotic drugs. *Br J Pharmacol* **138:**343–350.
Kulick MB and von Kügelgen I (2002) P2Y-receptors mediating an inhibition of the evoked entry of calcium through N-type calcium channels at neuronal processes. *J Pharmacol Exp Ther* **303:**520–526.
Marteau F, Le Poul E, Communi D, Communi D, Labouret C, Savi P, Boeynaems JM, and Gonzalez NS (2003) Pharmacological characterization of the human $P2Y_{13}$ receptor. *Mol Pharmacol* **64:**104–112.
Moskvina E, Unterberger U, and Boehm S (2003) Activity-dependent autocrine-paracrine activation of neuronal P2Y receptors. *J Neurosci* **23:**7479–7488.
North RA (2002) Molecular physiology of P2X receptors. *Physiol Rev* **82:**1013–1067.
Powell AD, Teschemacher AG, and Seward EP (2000) P2Y purinoceptors inhibit exocytosis in adrenal chromaffin cells via modulation of voltage-operated calcium channels. *J Neurosci* **20:**606–616.
Sak K and Webb TE (2002) A retrospective of recombinant P2Y receptor subtypes and their pharmacology. *Arch Biochem Biophys* **397:**131–136.
Simon J, Filippov AK, Goransson S, Wong YH, Frelin C, Michel AD, Brown DA, and Barnard EA (2002) Characterization and channel coupling of the $P2Y_{12}$ nucleotide receptor of brain capillary endothelial cells. *J Biol Chem* **277:**31390–31400.
Takasaki J, Kamohara M, Saito T, Matsumoto M, Matsumoto S, Ohishi T, Soga T, Matsushime H, and Furuichi K (2001) Molecular cloning of the platelet $P2T_{AC}$ ADP receptor: pharmacological comparison with another ADP receptor, the $P2Y_1$ receptor. *Mol Pharmacol* **60:**432–439.
Teschemacher AG and Seward EP (2000) Bidirectional modulation of exocytosis by angiontensin II involves multiple G-protein-regulated transduction pathways in adrenal chromaffin cells. *J Neurosci* **20:**4776–4785.
Unterberger U, Moskvina E, Scholze T, Freissmuth M, and Boehm S (2002) Inhibition of adenylyl cyclase by neuronal P2Y receptors. *Br J Pharmacol* **135:**673–684.
Vartian N and Boehm S (2001) P2Y receptor-mediated inhibition of voltage-activated Ca^{2+} currents in PC12 cells. *Eur J Neurosci* **13:**899–908.
Von Kügelgen I, Schoffel E, and Starke K (1989) Inhibition by nucleotides acting at presynaptic P2-receptors of sympathetic neuro-effector transmission in the mouse isolated vas deferens. *Naunyn-Schmiedeberg's Arch Pharmacol* **340:**522–532.
Wirkner K, Schweigel J, Gerevich Z, Franke H, Allgaier C, Barsoumian EL, Draheim H, and Illes P (2004) Adenine nucleotides inhibit recombinant N-type calcium channels via G protein-coupled mechanisms in HEK 293 cells: involvement of the $P2Y_{13}$ receptor-type. *Br J Pharmacol* **141:**141–151.
Zhang JM, Wang HK, Ye CQ, Ge W, Chen Y, Jiang Z l, Wu CP, Poo MM, and Duan S (2003) ATP released by astrocytes mediates glutamatergic activity-dependent heterosynaptic suppression. *Neuron* **40:**971–982.

Address correspondence to: Dr. Elizabeth P. Seward, Department of Biomedical Sciences, University of Sheffield, Alfred Denny Building, Western Bank, Sheffield, S10 2TN, United Kingdom. E-mail: e.p.seward@sheffield.ac.uk